

# Synthesis and Antiproliferative Activity of a New Series of Mono- and Bis(dimethylpyrazolyl)-s-triazine Derivatives Targeting EGFR/PI3K/AKT/mTOR Signaling Cascades

Ihab Shawish, Assem Barakat,\* Ali Aldalbahi, Azizah M. Malebari, Mohamed S. Nafie, Adnan A. Bekhit, Amgad Albohy, Alamgir Khan, Zaheer Ul-Haq, Matti Haukka, Beatriz G. de la Torre, Fernando Albericio,\* and Ayman El-Faham\*



Cite This: *ACS Omega* 2022, 7, 24858–24870



Read Online

ACCESS |



Metrics & More

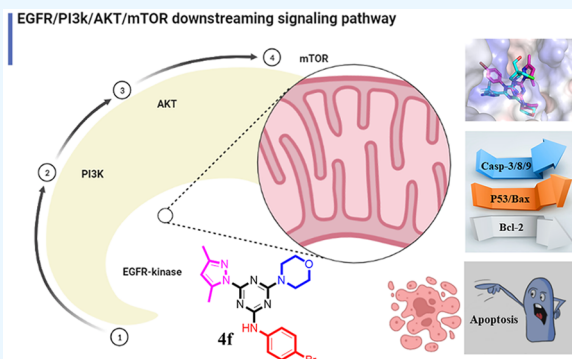


Article Recommendations



Supporting Information

**ABSTRACT:** Here, we synthesized a new series of *mono*- and *bis*(dimethylpyrazolyl)-s-triazine derivatives. The synthetic methodology involved the reaction of different mono- and dihydrazinyl-s-triazine derivatives with acetylacetone in the presence of triethylamine to produce the corresponding target products in high yield and purity. The antiproliferative activity of the novel *mono*- and *bis*(dimethylpyrazolyl)-s-triazine derivatives was studied against three cancer cell lines, namely, MCF-7, HCT-116, and HepG2. *N*-(4-Bromophenyl)-4-(3,5-dimethyl-1*H*-pyrazol-1-yl)-6-morpholino-1,3,5-triazin-2-amine **4f**, *N*-(4-chlorophenyl)-4,6-bis(3,5-dimethyl-1*H*-pyrazol-1-yl)-1,3,5-triazin-2-amine **5c**, and 4,6-bis(3,5-dimethyl-1*H*-pyrazol-1-yl)-*N*-(4-methoxyphenyl)-1,3,5-triazin-2-amine **5d** showed promising activity against these cancer cells: **4f** [(IC<sub>50</sub> = 4.53 ± 0.30 μM (MCF-7); 0.50 ± 0.080 μM (HCT-116); and 3.01 ± 0.49 μM (HepG2)]; **5d** [(IC<sub>50</sub> = 3.66 ± 0.96 μM (HCT-116); and 5.42 ± 0.82 μM (HepG2)]; and **5c** [(IC<sub>50</sub> = 2.29 ± 0.92 μM (MCF-7)]. Molecular docking studies revealed good binding affinity with the receptor targeting EGFR/PI3K/AKT/mTOR signaling cascades. Compound **4f** exhibited potent EGFR inhibitory activity with an IC<sub>50</sub> value of 61 nM compared to that of Tamoxifen (IC<sub>50</sub> value of 69 nM), with EGFR inhibition of 83 and 84%, respectively, at a concentration of 10 μM. Interestingly, **4f** showed remarkable PI3K/AKT/mTOR inhibitory activity with 0.18-, 0.27-, and 0.39-fold decrease in their concentration (reduction in controls from 6.64, 45.39, and 86.39 ng/mL to 1.24, 12.35, and 34.36 ng/mL, respectively). Hence, the synthetic 1,3,5-triazine derivative **4f** exhibited promising antiproliferative activity in HCT-116 cells through apoptosis induction by targeting the EGFR and its downstream pathway.



## INTRODUCTION

The widespread importance of the synthesis and modification of anticancer agents has given rise to many numbers of medicinal chemistry programs. In this regard, *s*-triazine derivatives have attracted attention due to their remarkable activity against a wide range of cancer cells.<sup>1–7</sup> Hexalen, also known as Altretamine (Figure 1, compound I), which was first approved by the U.S. Food and Drug Administration (U.S. FDA) in 1990, is an example of an antineoplastic drug based on an *s*-triazine privileged structure, and it is used for the treatment of refractory ovarian cancer.<sup>8</sup> Other examples of commercial drugs based on the *s*-triazine moiety include Enasidenib (Idhifa) (Figure 1, compound II), which is used to treat IDH2-positive acute leukemia and was first approved by the U.S. FDA in 2017,<sup>9</sup> and Gedatolisib (Figure 1, compound III), a first-in-class PI3K/mTOR inhibitor used to treat breast cancer.<sup>10</sup> Many other compounds carrying an *s*-triazine scaffold, including compounds IV<sup>11</sup> and V<sup>12</sup> for EGFR-TK

inhibitors, compound VI ZSTK474 (PI3K/MEK dual inhibitors),<sup>13</sup> compound VII, named Bimiralisib (PQR309),<sup>14–16</sup> and compound VIII as a dual inhibitor of PI3K/mTOR, have been reported as anticancer agents targeting EGFR/PI3K/AKT/mTOR cascades (Figure 1).<sup>17</sup>

The literature has reported other biological activities of *s*-triazine derivatives,<sup>18</sup> including antimicrobial,<sup>19</sup> antimalarial,<sup>20</sup> anti-inflammatory,<sup>21,22</sup> antibacterial and antifungal,<sup>11</sup> antioxidant, anticholinesterase,<sup>23,24</sup> and antiviral activity.<sup>25</sup> In this regard, *s*-triazine can be considered a promiscuous molecule. Beyond their biological activities, *s*-triazine derivatives have

Received: May 17, 2022

Accepted: June 22, 2022

Published: July 7, 2022



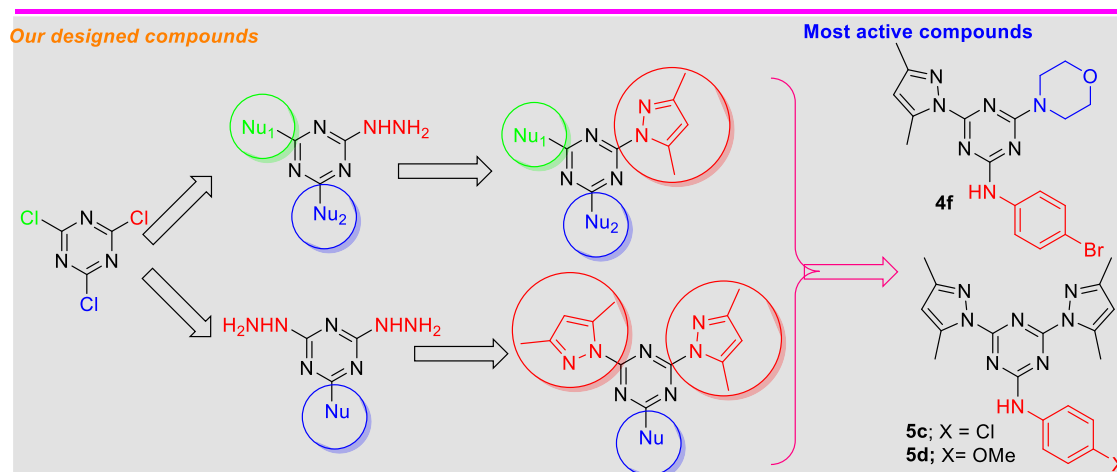
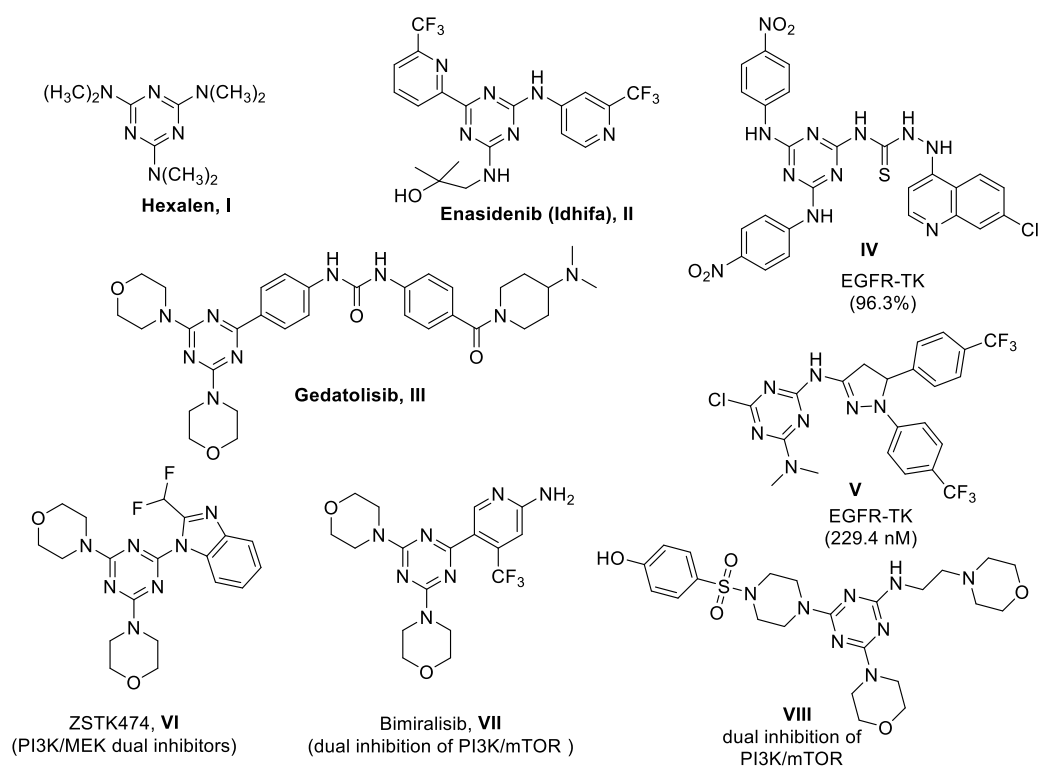


**Figure 1.** Selected *s*-triazine as an anticancer agent targeting EGFR/PI3K/AKT/mTOR cascades and our designed compounds.

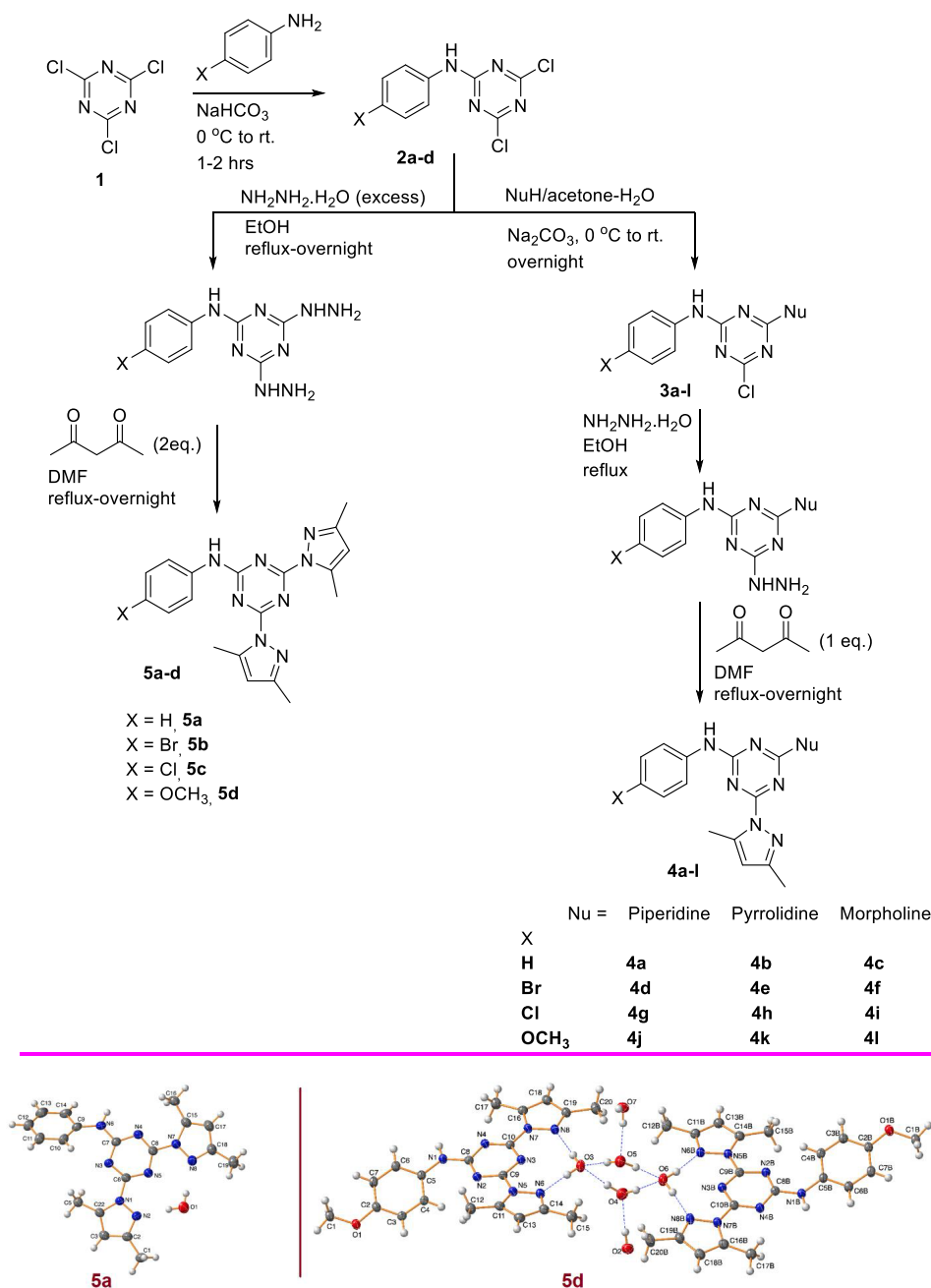
many applications in coordination chemistry<sup>26</sup> and as promising corrosion inhibitors.<sup>27</sup>

Furthermore, it has been reported that the combination of *s*-triazine derivatives with other significant bioactive moieties results in a prominent enhancement of their potential activity in various biological and pharmaceutical applications.<sup>28,29</sup> Pyrazole is one of the heterocyclic analogues that has a wide range of bioactivities, including anti-inflammatory, anticancer, antifungal, and antimicrobial activity, among others.<sup>30–33</sup> Many pyrazole-containing drugs have already been approved by the corresponding regulatory agencies and are widely used for various pharmacological and medicinal applications. Phenazone (analgesic and antipyretic), aminopyrine and aminophenazone (anti-inflammatory), and oxyphenbutazone (antipyretic, analgesic, anti-inflammatory, mild uricosuric) are representative examples of such drugs.<sup>33–37</sup> Synthesis of a new

class of compounds with pharmacophoric hybridization has received a lot of attention from researchers, as indicated in lower part of Figure 1, in which the designed molecules-based *s*-triazine with different pharmacophores was explored.

As a continuation of the promising anticancer properties shown by pyrazolyl-*s*-triazine derivatives synthesized in our previous research projects,<sup>28,35</sup> in the present study, a novel series of these derivatives (Figure 1) was synthesized, and their activity was tested against breast carcinoma (MCF-7), colorectal carcinoma (HCT-116), and liver carcinoma (HepG2) cells. Furthermore, a molecular docking study was performed targeting EGFR/PI3K/AKT/mTOR cascades. Finally, the EGFR enzymatic assay and the PI3k/AKT/mTOR downstream signaling pathway were assessed to confirm the computational study.

**Scheme 1. Synthetic Route of Mono- and Bispyrazolyl-*s*-triazine Derivatives and the X-ray Crystal Structures of Compounds 5a (CCDC 2163939) and 5d (CCDC 2163940)**

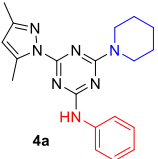
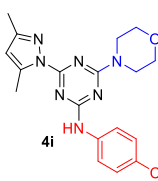
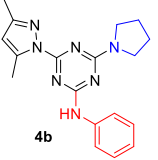
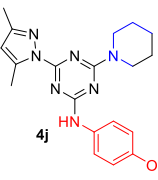
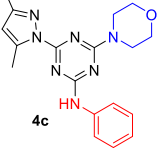
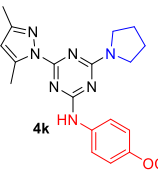
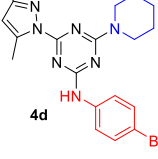
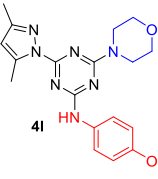
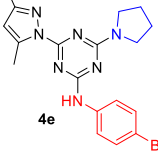
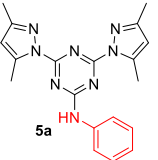
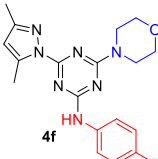
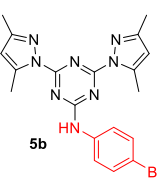
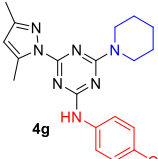
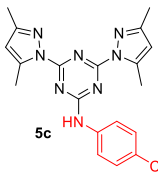
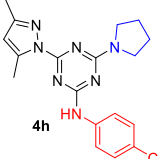
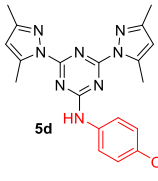


## RESULTS AND DISCUSSION

**Chemistry.** The initial derivatization step of cyanuric chloride 1 in this synthetic route was carried out via nucleophilic aromatic substitution of the chlorine atom by aromatic nitrogen-containing nucleophiles, such as aniline and *p*-substituted aniline, in the presence of an alkaline medium of sodium hydrogen carbonate as the hydrogen chloride receptor, following the previously reported method (Supporting Information (SI)).<sup>38</sup> The regioselectivity of this reaction was thermally optimized by performing the reaction at 0 °C to ensure the replacement of only one chlorine atom, leaving the two other chlorine units in the triazine moiety, which afforded the dichloro-monosubstituted-*s*-triazine derivatives 2a–d.

The second synthetic step involved a further displacing of one of the chlorine atoms in monosubstituted triazine derivatives 2a–d by aliphatic nitrogen-containing nucleophiles such as piperidine, pyrrolidine, and morpholine. The same synthetic methodology as the previous step (SI)<sup>38</sup> was applied, but the reaction time was increased to 12 h to overcome the deactivation behavior of the amino electron-donating group, which was inserted in the first step toward nucleophilic aromatic substitution. This approach afforded 2-chloro-4,6-disubstituted *s*-triazine derivatives 3a–l in good yield and purity, as indicated from the spectral data (SI). The monochloro 3a–l and dichloro 2a–d derivatives were then treated with hydrazine hydrate (80%) in EtOH overnight under reflux to afford the hydrazine derivatives, which, without further purification, reacted directly with acetylacetone in the

Table 1. Cytotoxicity Profile of Pyrazolyl-*s*-triazine Derivatives in Human Cancer Cell Lines<sup>a</sup>

Compound no.	IC <sub>50</sub> values (μM)			Compound no.	IC <sub>50</sub> values (μM)		
	MCF-7 cells	HCT-116 cells	HepG2 cells		MCF-7 cells	HCT-116 cells	HepG2 cells
 <b>4a</b>	13.71 ± 2.99	9.61 ± 2.28	9.32 ± 0.32	 <b>4i</b>	8.03 ± 0.11	5.21 ± 0.35	3.65 ± 1.62
 <b>4b</b>	7.15 ± 0.78	10.06 ± 1.30	8.23 ± 1.17	 <b>4j</b>	2.93 ± 1.11	4.85 ± 1.76	11.77 ± 1.49
 <b>4c</b>	18.63 ± 0.78	12.42 ± 0.97	8.61 ± 0.92	 <b>4k</b>	3.76 ± 0.52	3.45 ± 2.31	6.72 ± 0.67
 <b>4d</b>	27.74 ± 3.19	30.31 ± 2.42	15.73 ± 4.29	 <b>4l</b>	18.62 ± 0.80	2.26 ± 0.94	15.26 ± 2.56
 <b>4e</b>	7.32 ± 0.33	32.24 ± 3.33	3.81 ± 0.67	 <b>5a</b>	10.75 ± 1.40	3.17 ± 1.10	4.64 ± 0.36
 <b>4f</b>	4.53 ± 0.30	0.50 ± 0.080	3.01 ± 0.49	 <b>5b</b>	2.66 ± 1.65	10.40 ± 2.54	5.60 ± 1.24
 <b>4g</b>	8.65 ± 0.69	2.42 ± 0.90	6.33 ± 2.23	 <b>5c</b>	2.29 ± 0.92	11.04 ± 1.62	19.50 ± 8.06
 <b>4h</b>	7.87 ± 1.39	2.17 ± 0.32	4.35 ± 0.99	 <b>5d</b>	11.97 ± 1.68	3.66 ± 0.96	5.42 ± 0.82
				<b>Tamoxifen</b>	5.12 ± 0.36	26.41 ± 4.11	2.45 ± 0.20

<sup>a</sup>Values are expressed as mean ± SD of three independent trials. Tamoxifen was used as the control.

presence of triethylamine and DMF as solvent following the method reported by our group and others<sup>35,37,38</sup> to render the target products **4a–l** and **5a–d**, respectively (Scheme 1) (Material and methods, SI). The chemical structures for all of

the new synthesized compounds were assigned based on different spectroscopic tools including NMR, MS, IR, and CHN analysis. Indeed, single-crystal X-ray diffraction analysis of compounds **5a** and **5d** further confirmed their structures

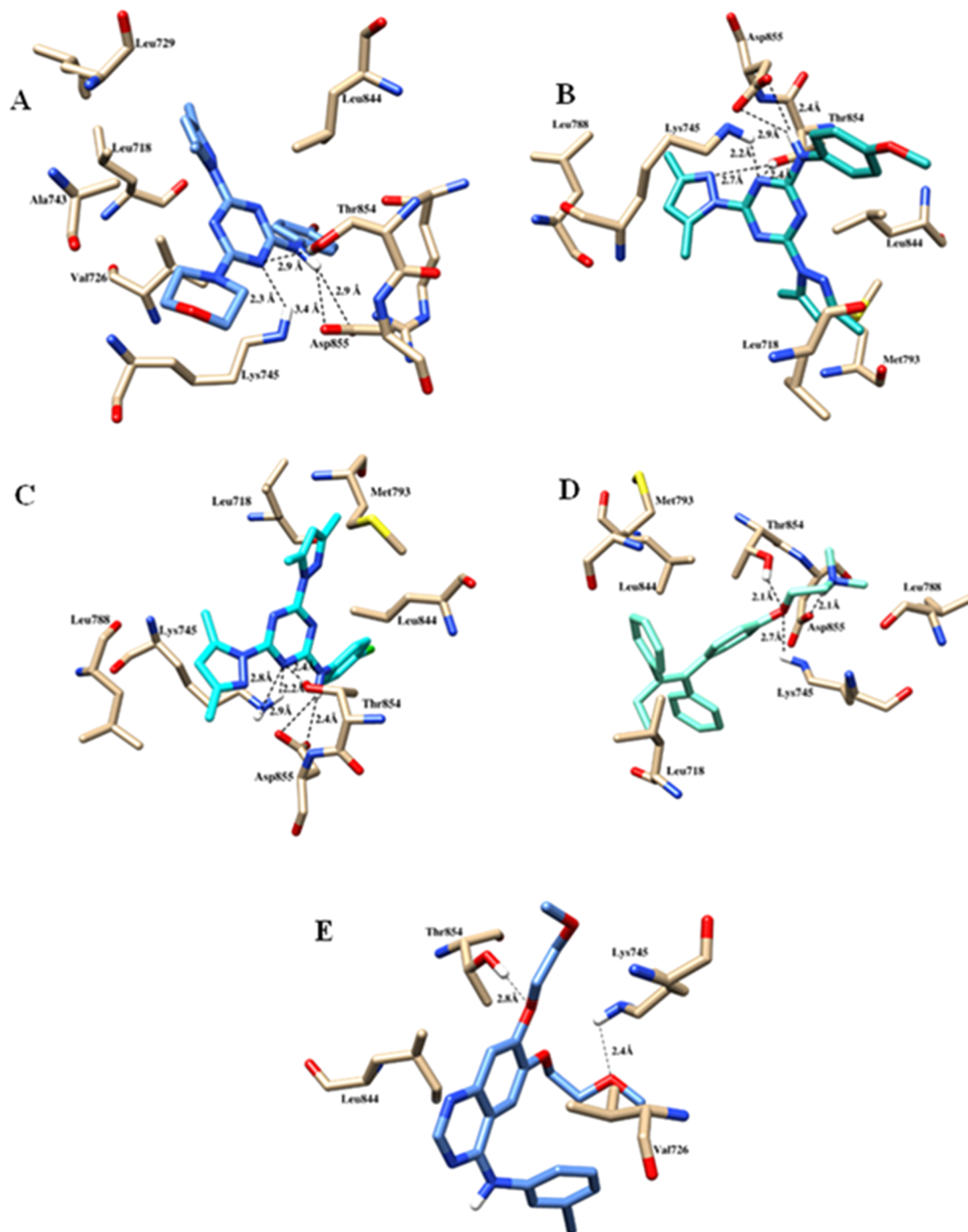


**Figure 2.** Dock poses and binding interactions of (A) **4f**, (B) **5d**, (C) **5c**, (D) Tamoxifen, and (E) Erlotinib.

(Table S1, SI). The crystal data and refinement details are summarized in Table S1, while the X-ray structure showing thermal ellipsoids drawn at the 30% probability level is shown in Scheme 1. Both structures crystallized in the triclinic crystal system and  $P\bar{1}$  space group. The structure of **5d** comprised one molecule of the organic target compound and one crystal water, which represents the asymmetric formula of the structure leading to  $z = 2$ . On the other hand, the asymmetric formula of **5a** comprised two molecules of the target compound and six water molecules, leading to  $z = 4$ . In the former, the two pyrazolyl moieties are twisted from the mean plane of the *s*-triazine core mean plane by 14.36 and 5.18° for

the pyrazole groups N1N2C2C3C22 and N8N7C15C17C18, respectively, while in the latter, the corresponding value does not exceed 11.17°. In addition, the phenyl group of the aniline moiety creates a twist angle of 38.09°, with the *s*-triazine core mean plane of **53**. The corresponding values for **52** are 14.25 and 23.29°.

**Biology. In Vitro Antiproliferative Assay.** In our previous publication,<sup>35</sup> we reported a series of *mono*- and *bis*-pyrazolyl-*s*-triazine derivatives incorporating piperidine and morpholine on the triazine ring and studied their effects on human breast cancer (MCF-7 and MDA-MB-231), human liver carcinoma (HepG2), human colorectal carcinoma (LoVo), and human

**Table 2. Docking Scores of Target Compounds against PI3K and mTOR**

ligand	docking score(kcal/mol)	
	PI3K (5JHB)	mTOR (4JSV)
4a	−9.4	−8
4b	−9.1	−7.7
4c	−9.3	−8
4d	−9.1	−7.8
4e	−9.1	−7.8
4f	−8.9	−7.7
4g	−9.1	−7.8
4h	−8.9	−8
4i	−9	−7.7
4j	−8.5	−8
4k	−8.9	−7.9
4l	−8.7	−7.9
5a	−9.8	−8.6
5b	−9.2	−8
5c	−9.1	−8
5d	−9.7	−8.1
cocrystallized ligand	−9.1	−6.9

leukemia (K562) cell lines. Most of the reported triazine derivatives<sup>35</sup> showed weak to moderate activity against the four cell lines. As a continuation of our interest in pyrazolyl-s-triazine derivatives, here, we constructed aniline and *p*-substituted aniline as the hydrophobic tail in the newly synthesized pyrazolyl-s-triazine derivatives and assessed these compounds against breast cancer (MCF-7), colon carcinoma (HCT-116), and liver carcinoma (HepG2). Lipophilicity in the tested compounds improved the EGFR-based cytotoxicity against the tested cancer cell lines. This may be due to the lipophilic moieties in the EGFR binding sites that enhanced their binding affinities and hence the stability of compound–protein complexes. The synthesized triazine compounds **4a–l** and **5a–d** affected the viability of the three cell lines (moderate to strong), as determined by the MTT cell viability assay (Table 1). To explain the cytotoxicity of the compounds and to better understand the structure–activity relationship, we would classify them into the following two categories: group A: **4a–l**, which have the monopyrazole/anilino derivatives/amine derivatives; and group B: **5a–d**, which have a bispyrazoles/anilino derivative-based triazine nucleus.

The results for group A (monopyrazolyl-s-triazine derivatives), **4a–l**, are shown in Table 1. In summary, the compounds exhibited IC<sub>50</sub> values (μM) ranging from 2.93 to 27.74 μM in the breast cancer cell line (MCF-7). The most active hybrid in this series was **4j** (IC<sub>50</sub> = 2.93 ± 1.11 μM), whose chemical structure comprised monopyrazole/*p*-MeO-anilino and piperidine as pending groups of the triazine core structure. By switching the methoxy group as the electron-donating group on the aniline ring for an electron-withdrawing atom such as Cl (compound **4g**) or Br (compound **4d**), the activity decreased to 8.65 ± 0.69 and 27.74 ± 3.19 μM, respectively. Also, this effect was observed for the unsubstituted aniline ring, as indicated in **4a** (IC<sub>50</sub> = 13.71 ± 2.99 μM). The introduction of the morpholine ring, such as in compounds **4c** (IC<sub>50</sub> = 18.63 ± 0.78 μM) and **4l** (IC<sub>50</sub> = 18.62 ± 0.80 μM), in place of the piperidine in the structure, such as in compounds **4a** (IC<sub>50</sub> = 13.71 ± 2.99 μM) and **4j** (IC<sub>50</sub> = 2.93 ± 1.11 μM), did not improve cytotoxicity, except compound **4f** showed higher cytotoxicity with IC<sub>50</sub> = 4.53 ±

0.30 μM compared to that of compound **4d** (27.74 ± 3.19 μM) (Table 1). Switching from a six-membered (piperidine or morpholine) pyrrolidine ring to a five-membered ring led to improved activity, as shown with **4k**, **4b**, **4e**, and **4h** (Table 1). For example, compound **4b** (IC<sub>50</sub> = 7.15 ± 0.78 μM) is greater than compounds **4a** (IC<sub>50</sub> = 13.71 ± 2.99 μM) and **4c** (IC<sub>50</sub> = 18.63 ± 0.78), also as observed in compound **4e** (IC<sub>50</sub> = 7.32 ± 0.33 μM), which is more active than **4d** (IC<sub>50</sub> = 27.74 ± 3.19 μM); meanwhile, compound **4k** (IC<sub>50</sub> = 3.76 ± 0.52 μM) is more potent than **4l** (IC<sub>50</sub> = 18.62 ± 0.80 μM). Again, the *p*-methoxy derivatives showed more potency than *p*-chloro-, *p*-bromo-, and the unsubstituted derivatives and even greater potency than the control Tamoxifen against the breast cancer cell line (MCF-7).

On the other hand, regarding the colon carcinoma cell line (HCT-116), **4a–l** showed IC<sub>50</sub> values ranging from 0.50 to 32.24 μM. The most active hybrid in this series was **4f** (IC<sub>50</sub> = 0.50 ± 0.08 μM), whose chemical structure comprised monopyrazole/*p*-Br-anilino and a morpholine motif based on the triazine core structure and was compared to monopyrazole/*p*-Br-anilino and piperidine **4d** (IC<sub>50</sub> = 30.31 ± 2.42 μM) or pyrrolidine **4e** (IC<sub>50</sub> = 32.24 ± 3.33 μM) (Table 1). By keeping the morpholine ring along with the pyrazole ring and changing the substituents on the aniline, the results indicated that compound **4l** (MeO group) showed more activity than **4i** (Cl-atom) and **4c** (H) (Table 1).

Group A **4a–l** showed activity against the liver carcinoma cell line (HepG2), with IC<sub>50</sub> values ranging from 3.01 ± 0.49 to 15.73 ± 4.29 μM. Again, the most active hybrid in this series was **4f** (IC<sub>50</sub> = 3.01 ± 0.49 μM) (mono-pyrazole/*p*-Br-anilino and morpholine as triazine pending substituents) compared to its analogues (monopyrazole/*p*-Br-anilino and piperidine **4d** or pyrrolidine **4e** as triazine pending substituents) as in the case of HCT-116.

Group B (*bis*-pyrazolyl-s-triazine derivatives) **5a–d** showed activity against the breast cancer cell line (MCF-7), with IC<sub>50</sub> values ranging from 2.29 ± 0.92 to 11.97 ± 1.68 μM (Table 1). The most active hybrid in this series was **5c** (two *bis*-pyrazoles and *p*-Cl-anilino as substituents of the triazine). Replacement of the *p*-Cl-anilino with the *p*-Br-anilino in **5b** did not greatly alter its activity. In contrast, the unsubstituted (compound **5a**) or *p*-methoxy group as the electron-donating group (compound **5d**) led to a decrease in activity (Table 1). On the other hand, **5a** and **5d** showed greater activity against the colon carcinoma cell line (HCT-116) than did the *p*-bromo derivatives, as reflected by their IC<sub>50</sub> values (Table 1). In the case of the liver carcinoma cell line (HepG2), **5a**, **5b**, and **5d** exhibited similar activity, and **5c** showed the least activity in this series, with an IC<sub>50</sub> of 19.50 ± 8.06 μM (Table 1).

**Molecular Docking Analysis.** Molecular docking studies were used to study the possible binding model and specifics of the interaction mechanism between the synthetic compounds and target protein EGFR and as a valuable method to graphically illustrate the changes in the interaction between the receptor and ligand. MOE (molecular operating environment) was used to conduct molecular docking studies to examine the target compounds' binding association and interaction with the active site residues such as Lys745, Met790, Asn842, and Asp855 of the EGFR kinase protein.<sup>39</sup> All of the compounds (Table 1) were docked to the target protein EGFR. The docking score of the compounds was used to assess their binding affinities. Those that showed the highest binding

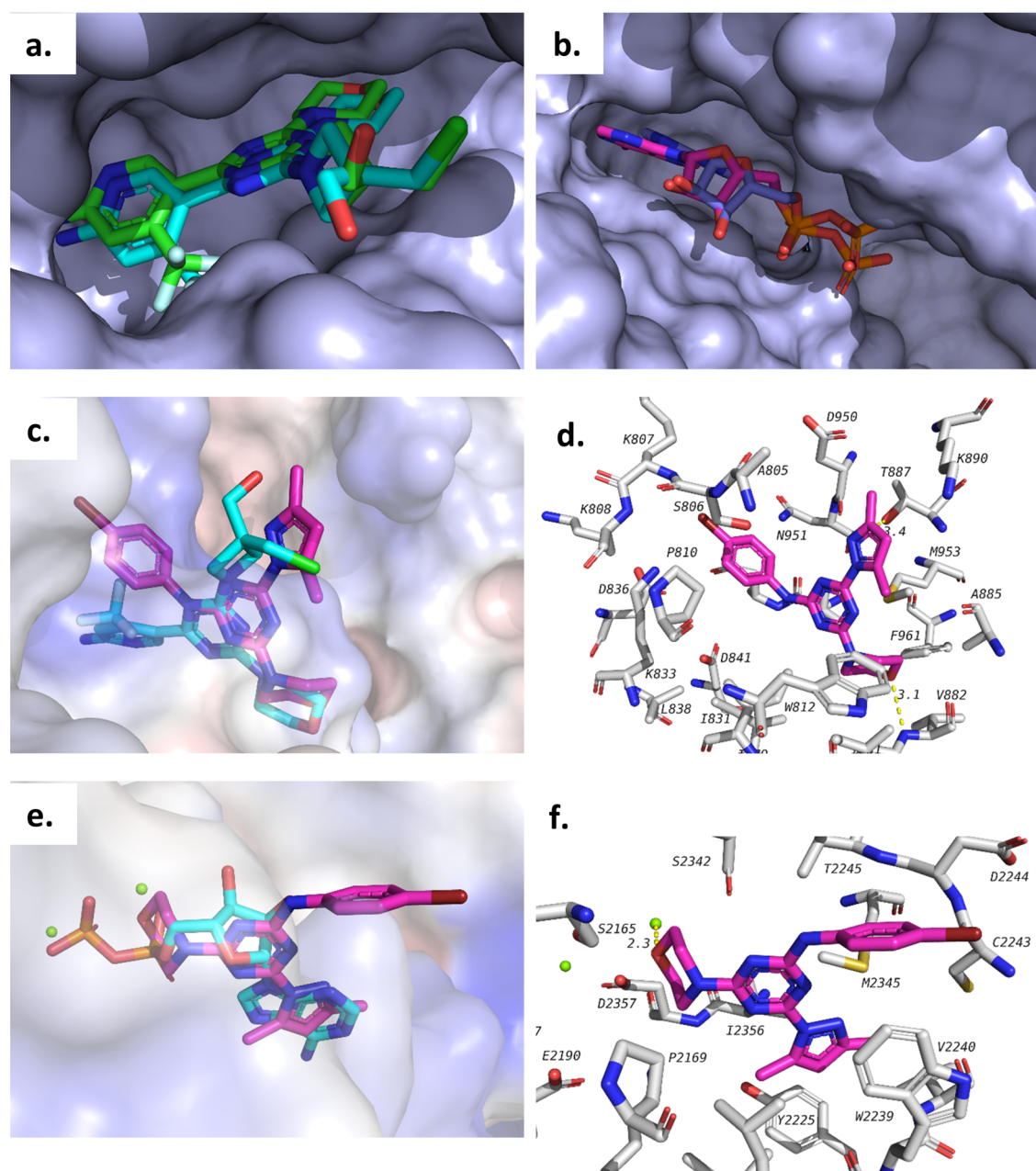


**Figure 3.** (a) Validation of PI3K (SJHB) showing cocrystallized ligand (blue) overlapped with docked structure (green). (b) Validation of mTOR (4JSV) showing cocrystallized ligand (blue) overlapped with docked structure (pink). (c) Docking pose of **4f** (pink) in PI3K active site overlapped with cocrystallized ligand (blue). (d) Interactions of **4f** (pink) in PI3K active site. (e) Docking pose of **4f** (pink) in mTOR active site overlapped with cocrystallized ligand (blue). (f) Interactions of **4f** (pink) in mTOR active site. Magnesium ions in the active site are shown as green spheres.

affinity to EGFR (Figure 2) and best interactions were **4f**, **5c**, **5d**, Tamoxifen, and Erlotinib. The results show that the selected docked compounds had strong binding affinities with the target protein PDB ID 6V6O, with a docking score of  $-7.49$  to  $-8.82$  kcal/mol. Docking analysis revealed that Lys745, Thr854, and Asp855 are in the binding pocket of a protein that plays a pivotal role in the binding mode of the ligand with the receptor. The docking scores of EGFR with compounds **4f**, **5c**, **5d**, Erlotinib, and Tamoxifen were  $-8.26$ ,  $-8.82$ ,  $-8.68$ – $8.51$ , and  $-7.49$ , respectively. Binding interaction analysis revealed that each of the selected compounds has hydrogen bonding with Lys745, Thr854, and Asp855. In five promising compounds, standard Erlotinib and Tamoxifen formed two and three hydrogen bonding interactions,

respectively, while test compounds **4f** and **5d** have four and **5c** demonstrates five hydrogen bonding interactions (Figure 2).

Hence, the molecular docking results of binding affinities of **4f**, **5d**, and **5c** toward EGFR were consistent with the experimental enzymatic inhibition and the cytotoxic activity observed. Analysis of the PI3K/AKT/mTOR pathway showed the tested compounds exhibited promising inhibitory activities downstream. These results are consistent with the findings of Singh and co-workers,<sup>40</sup> who discovered some novel triazine derivatives via attenuated EGFR and PI3K/AKT/mTOR activities.

**Potential Inhibition of PI3K and mTOR with Novel Trisubstituted Triazine Derivatives.** Most of the com-

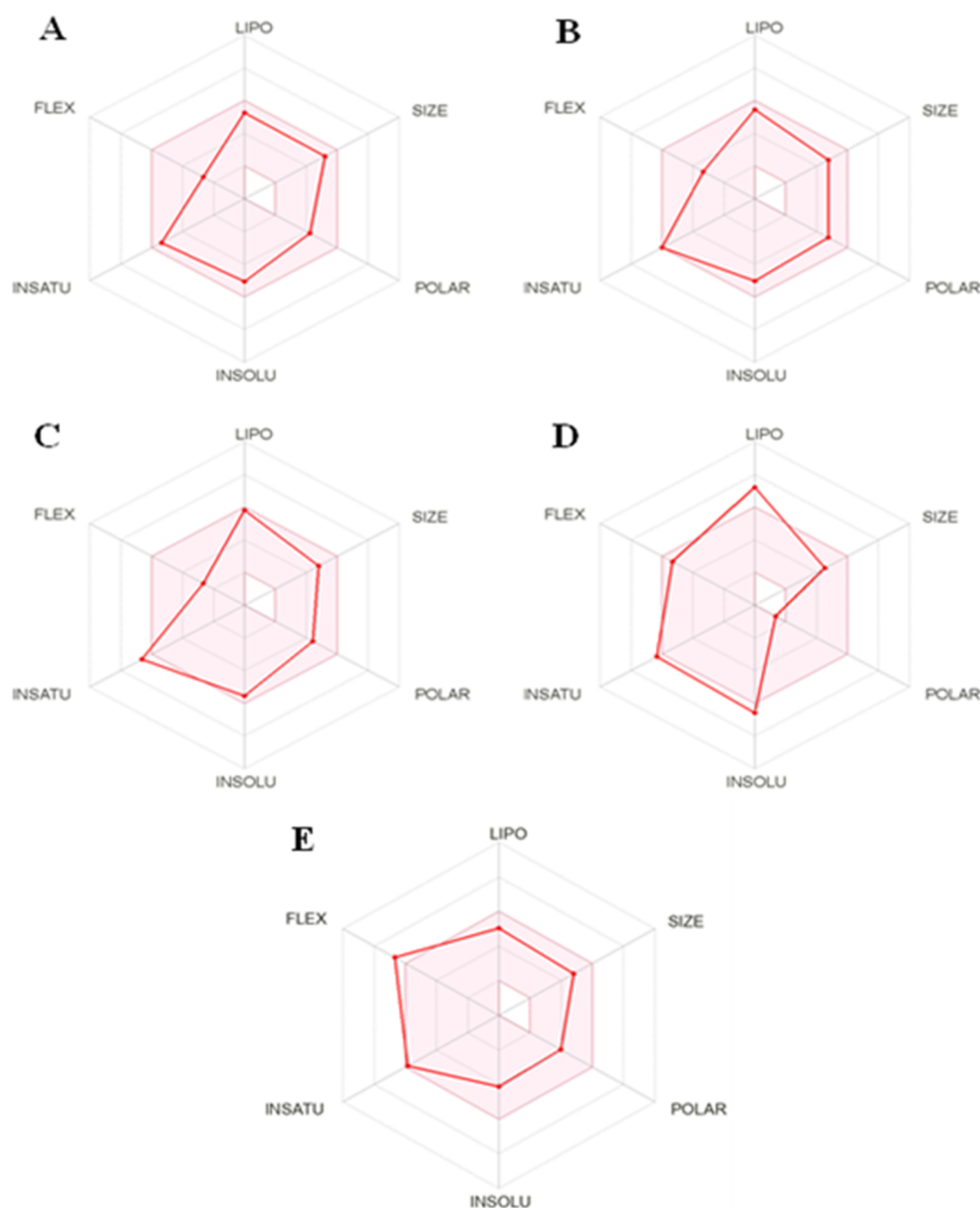


**Figure 4.** Bioavailability radar of selected compounds: (A) **4f**, (B) **5d**, (C) **5c**, (D) Tamoxifen, and (E) Erlotinib.

**Table 3. Physicochemical Properties of Selected Ligands**

S. No	properties	<b>4f</b>	<b>5d</b>	<b>5c</b>	Tamoxifen	Erlotinib
1	molecular weight (g/mol)	430.30	390.44	394.86	372.52	399.44
2	no. of heavy atoms	27	29	28	28	29
3	no. aromatic heavy atoms	17	22	22	18	16
4	rotatable bonds	4	5	4	8	10
5	H-bond acceptor	5	6	5	1	6
6	H-bond donor	1	1	1	1	1
7	TPSA	80.99 Å <sup>2</sup>	95.57 Å <sup>2</sup>	86.34 Å <sup>2</sup>	13.67 Å <sup>2</sup>	74.73 Å <sup>2</sup>

pounds showed potent inhibition of MCF-7, HCT-116, and HepG2 cancer cells. We sought to study potential enzymatic targets of these compounds through target fishing. To this end, we searched for potential targets of the most potent structure, **4f**, using two online servers. The first, SwissTargetPredict, revealed several kinases as the top hits for this compound. Among these, phosphatidylinositol-3-kinase (PI3K) and mammalian target of rapamycin (mTOR) were the top two

predicted based on the probability and number of similar compounds in 2D and 3D structures. Of note, mTOR is a component of the protein kinase B (PKB) pathway, and it acts downstream of PI3K in that pathway.<sup>41</sup> Dual inhibition of PI3K and mTOR is a known strategy used to fight cancer, and morpholino triazine is a scaffold that inhibits both targets.<sup>42</sup> Given these considerations, we used molecular docking to study the potential binding modes of our compounds with the

**Table 4.** IC<sub>50</sub> of the Activity of the Tested Compounds against EGFR-PK Assay

compound	autophosphorylation percentage inhibition at conc (10 $\mu$ M)	EGFR PK inhibition, IC <sub>50</sub> (nM) <sup>a</sup>
4f	82.6 $\pm$ 2.38	61 $\pm$ 0.002
5c	69.68 $\pm$ 2.01	102 $\pm$ 0.004
5d	74.68 $\pm$ 2.47	98 $\pm$ 0.003
Erlotinib	83.89 $\pm$ 3.26	78.65 $\pm$ 3.54

<sup>a</sup>Values are expressed as mean  $\pm$  SD of three independent replicates. IC<sub>50</sub> values were calculated using a sigmoidal nonlinear regression curve fit of percentage inhibition against five concentrations of each compound.

two target proteins (Table 2). Target proteins were downloaded from the Protein Data Bank (PDB) under codes 5HJB for PI3K and 4JSV for mTOR. Code 5JHB is a crystal structure of PI3K cocrystallized with a potent inhibitor that has the morpholino triazine scaffold. Redocking of the cocrystallized ligand was done for validation purposes. The software was able to predict the correct pose with good accuracy and a root-mean-square deviation (RMSD) of 1.149 Å, as predicted by DockRMSD (Figure 3a). Code 4JSV, on the other hand, is the crystal structure of mTOR cocrystallized with ADP, which indicates an ATP binding site. Validation of this target gave an RMSD of 1.642 Å, which is within an acceptable range (<2 Å) (Figure 3b). Docking scores revealed (Table 2) the test compounds showed greater binding to PI3K compared to mTOR, with differences reaching about 1.6 kcal/mol. Among each target, the energy differences were not large and most of the compounds showed similar binding modes. In terms of

binding pose and interaction, the test compounds bound to PI3K in a similar manner as the morpholino triazine cocrystallized ligand. In fact, derivatives with a morpholino triazine moiety such as 3f, the best compound in the biological evaluation, showed good overlap with the cocrystallized ligand (Figure 3c). Compound 4f conserved the hydrogen bond between the oxygen atom of its morpholine ring and V882, similar to what was observed for the cocrystallized ligand. Furthermore, 4f showed another hydrogen bond with T887. In addition, several hydrophobic interactions were maintained, such as those with P810, W812, V882, and F961 (Figure 3d). Docking of the test compounds in the ATP binding site of mTOR showed good overlap with ADP, which was cocrystallized with the protein, as seen with 4f as an example (Figure 3e). The pyrazole ring of 4f overlapped with the adenine ring of ADP. Also, the oxygen atom of the morpholino ring was in proximity to one of the magnesium ions present in the active site, as well as several hydrophobic interactions (Figure 3f). These results suggest that our test compounds have potential inhibitory capacity over PI3K and possibly over mTOR. These compounds thus require further attention.

**ADME Analysis.** The prediction of the physicochemical and pharmacokinetic properties of the selected compounds (as described above) from docking results was explored. The ADME results showed six physicochemical properties, namely, lipophilicity, size, polarity, solubility, saturation, and flexibility. From Figure 4, A–E denotes 4f, 5c, 5d, Tamoxifen, and Erlotinib, respectively.

All six physicochemical properties were in the validated range for compounds 4f and 5c. While in compound 5d,

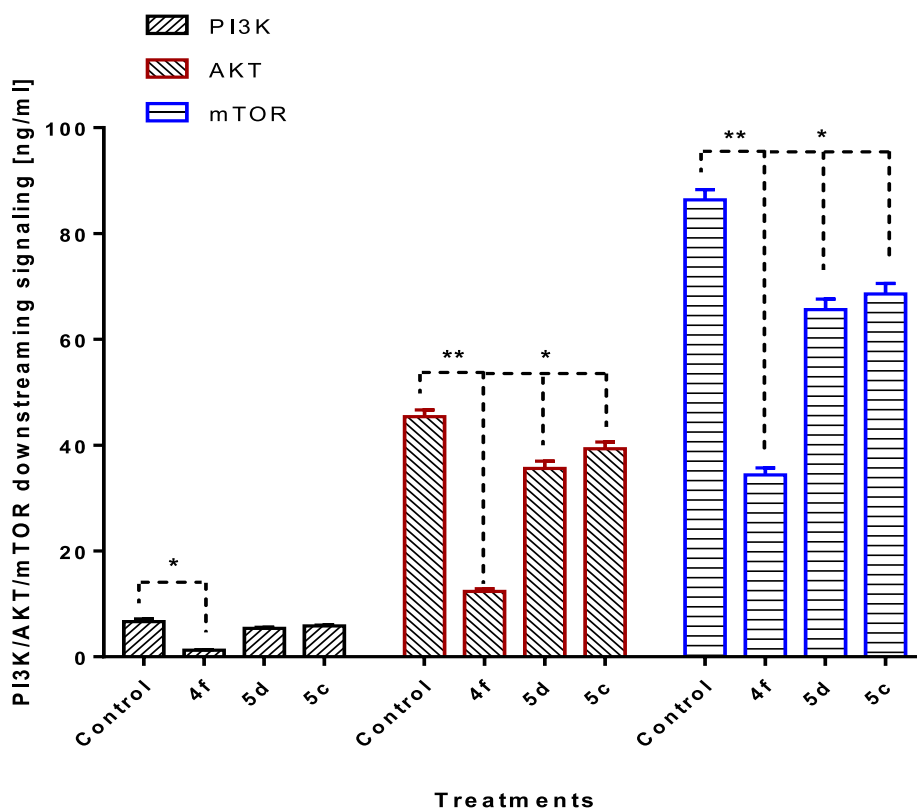


**Figure 5.** Activity of compounds 4f, 5d, and 5c against the EGFR downstream signaling pathway (PI3K/AKT/mTOR) in untreated and treated HCT-116 cells. Values are expressed as mean  $\pm$  SD of three independent replicates. \* $P$  < 0.05, \*\* $P$  < 0.001 significant difference between control and treated group using unpaired  $t$ -test.

Table 5. Fold Change of Apoptosis-Related Genes in Untreated and Treated HCT-116 Cells<sup>a</sup>

sample	fold change = $2^{-\Delta\Delta CT}$								
	proapoptotic gene					antiapoptotic and downstream genes			
	P53	Bax	Casp-3	Casp-8	Casp-9	Bcl-2	PI3K	AKT	mTOR
4f treated HCT-116	8.73 ± 0.79	6.54 ± 0.37	9.36 ± 0.67	1.69 ± 0.31	7.54 ± 0.69	0.24 ± 0.01	0.31 ± 0.02	0.27 ± 0.01	0.34 ± 0.03
untreated HCT-116	1								

<sup>a</sup>Values are expressed as mean ± SD of three independent replicates. Data were normalized using  $\beta$ -actin as the house-keeping gene.

instauration was slightly outside the validated range. Finally, for Tamoxifen, three physicochemical properties, namely flexibility, size and polarity, were in the validated range (Figure 4D), while three others lipophilicity, saturation and solubility fell outside the range. For Standard Erlotinib (Figure 4E) all five physicochemical properties in range except flexibility property. Some other physicochemical properties are also listed in Table 3.

**EGFR Enzymatic Assay.** Compounds 4f, 5c, and 5d were tested for their inhibitory capacity against EGFR. Compound 4f exhibited potent inhibitory activity; EGFR had an IC<sub>50</sub> value of 61 nM compared to that of Erlotinib, with an IC<sub>50</sub> value of 69 nM, with EGFR inhibition of 83 and 84%, respectively, at a concentration 10  $\mu$ M (Table 4). 5d and 5c showed moderate activity, with IC<sub>50</sub> values of 98 and 102 nM and EGFR inhibition of 74.7 and 70%, respectively.

**PI3K/AKT/mTOR Downstream Signaling Pathway.** The EGFR/PI3K/AKT/mTOR signaling cascade is important in many cellular processes, including cell growth and proliferation, apoptosis, survival, and metabolism, all of which contribute to tumor progression.<sup>43–45</sup> To study the effective molecular targets of the promising 4f, 5d, and 5c, which showed the highest cytotoxic activity against HCT-116 cells and promising EGFR inhibition, these compounds were tested against the PI3K/AKT/mTOR pathway.

The three compounds exhibited promising inhibitory activity against this pathway. Interestingly, 4f showed remarkable activity against PI3K/AKT/mTOR, reducing the concentrations in the control condition from 6.64, 45.39, and 86.39 ng/mL to 1.24, 12.35, and 34.36 ng/mL, respectively (Figure 5).

**Compound 4f Affected Apoptosis-Related Genes in Treated HCT-116 Cells.** Both untreated and treated HCT-116 cells were subjected to RT-PCR to validate apoptosis in the PI3K/AKT/mTOR pathway. Treatment with 4f increased the expression of proapoptotic genes and decreased that of antiapoptotic genes (Table 5). This treatment led to an increase in p53, Bax, caspases-3, -8, and -9, which showed a fold of change of 8.73, 6.54, 9.36, 1.69, and 7.54, respectively. At the same time, 4f treatment caused a decrease in Bcl-2, with a 0.24-fold change as the antiapoptotic gene. Additionally, treatment with this compound inhibited the PI3K/AKT/mTOR downstream pathway, which showed a 0.31-, 0.27-, and 0.34-fold reduction in expression, respectively.

## MATERIALS AND METHODS

Unless stated otherwise, reagents were obtained from commercial sources, such as Sigma-Aldrich (Chemie GmbH, Taufkirchen, Germany), and used without further purification. The synthesized compounds were fully characterized. Thin-layer chromatography (TLC) was performed on Merck silica gel 60 F254, 20 × 20 cm plates, and visualized using a 254 nm

UV lamp. A standard rotary evaporator was used for vacuumed removal of the solvents. <sup>1</sup>H and <sup>13</sup>C NMR spectra were recorded in CDCl<sub>3</sub> and DMSO-*d*<sub>6</sub> on a JEOL spectrometer (JEOL, Tokyo, Japan) (400 or 500 MHz). Infrared spectra were recorded on a Thermo Scientific Nicolet iS10 FT-IR spectrometer (Thermo Fisher Scientific, Waltham, MA, USA). X-ray diffraction data were collected on a Rigaku Oxford Diffraction Supernova diffractometer and processed with CrysAlisPro software v. 1.171.41.93a (Rigaku Oxford Diffraction, Yarnton, UK, 2020) using Cu K $\alpha$  radiation.

**General Procedure for the Synthesis of Mono- and Bispyrazolyl-*s*-triazine Derivatives.** Mono-pyrazolyl-*s*-triazine derivatives 4a–l and bis-pyrazolyl-*s*-triazine 5a–d were prepared from the reaction of the hydrazine-*s*-triazine derivatives with acetylacetone in the presence of triethylamine as a base following the methods reported by our group and others<sup>28,35,37,38</sup> to give the desired products in good yield and purity (Material and Methods, SI).

## CONCLUSION

In summary, we synthesized new mono- and bis(dimethylpyrazolyl)-*s*-triazine derivatives and studied their activity against the MCF-7, HCT116, and HepG2 cancer cell lines. All of the compounds showed moderate to good cytotoxicity against the three lines in comparison to Tamoxifen as the control. Of these compounds, 4f, 4j, 4k, 5b, and 5c showed potent activity against MCF-7 cells, showing an IC<sub>50</sub> between 2.29 and 5.53  $\mu$ M, which is a similar but lower value than that of Tamoxifen (IC<sub>50</sub> 5.12 ± 0.36  $\mu$ M). Almost all of the tested compounds showed potent activity against the HCT-116 cell line compared to that of the control, and 4f showed excellent potency (IC<sub>50</sub> of 0.50 ± 0.080  $\mu$ M). Compounds 4e, 4f, 4h, 4i, 5a, 5b, 5c, and 5d displayed potent activity against the HepG2 cell line (IC<sub>50</sub> between 3.01 and 5.60  $\mu$ M) and thus activity similar to that of Tamoxifen (IC<sub>50</sub> 2.45 ± 0.20  $\mu$ M). Based on the docking studies' scores, we selected 4f, 5c, 5d, Erlotinib, and Tamoxifen for further molecular docking studies. The binding interaction analysis and examination of physicochemical properties revealed that 4f, 5c, and 5d outperformed Erlotinib and Tamoxifen. Following the molecular target, 4f exhibited potent EGFR inhibitory activity, with an IC<sub>50</sub> value of 61 nM (Tamoxifen, IC<sub>50</sub> = 69 nM). Additionally, for the downstreaming pathway of PI3K/AKT/mTOR, 4f showed remarkable inhibitory activity, reducing the expression of these genes 0.18-, 0.27-, and 0.39-fold, respectively. Finally, 4f induced apoptosis in HCT-116 cells by upregulating the proapoptotic genes p53, Bax, and caspase-3, -8, and -9, while it downregulated the antiapoptotic gene Bcl-2. We conclude that novel mono- and bis(dimethylpyrazolyl)-*s*-triazine derivatives are potent inhibitors of EGFR/PI3K/AKT/mTOR.

## ■ ASSOCIATED CONTENT

### SI Supporting Information

The Supporting Information is available free of charge at <https://pubs.acs.org/doi/10.1021/acsomega.2c03079>.

Synthesis and characterization of the synthesized compounds; copies of the spectra; X-ray crystal data; biology assays and molecular docking protocols (PDF)

X-ray data for **5a** (ZIP)

X-ray data for **5d** (ZIP)

## ■ AUTHOR INFORMATION

### Corresponding Authors

**Fernando Albericio** – Peptide Science Laboratory, School of Chemistry and Physics, University of KwaZulu-Natal, Durban 4000, South Africa; Institute for Advanced Chemistry of Catalonia (IQAC-CSIC), 08034 Barcelona, Spain; CIBER-BBN, Networking Centre on Bioengineering, Biomaterials and Nanomedicine, and Department of Organic Chemistry, University of Barcelona, 08028 Barcelona, Spain; [orcid.org/0000-0002-8946-0462](https://orcid.org/0000-0002-8946-0462); Email: [albericio@ukzn.ac.za](mailto:albericio@ukzn.ac.za)

**Ayman El-Faham** – Department of Chemistry, Faculty of Science, Alexandria University, Alexandria 21321, Egypt; [orcid.org/0000-0002-3951-2754](https://orcid.org/0000-0002-3951-2754); Email: [ayman.elfaham@alexu.edu.eg](mailto:ayman.elfaham@alexu.edu.eg), [aymanel\\_faham@hotmail.com](mailto:aymanel_faham@hotmail.com)

**Assem Barakat** – Department of Chemistry, College of Science, King Saud University, Riyadh 11451, Saudi Arabia; [orcid.org/0000-0002-7885-3201](https://orcid.org/0000-0002-7885-3201); Email: [ambarakat@ksu.edu.sa](mailto:ambarakat@ksu.edu.sa)

### Authors

**Ihab Shawish** – Department of Chemistry, College of Science, King Saud University, Riyadh 11451, Saudi Arabia; Department of Math and Sciences, College of Humanities and Sciences, Prince Sultan University, Riyadh 11586, Saudi Arabia

**Ali Aldalbahi** – Department of Chemistry, College of Science, King Saud University, Riyadh 11451, Saudi Arabia; [orcid.org/0000-0003-1644-2367](https://orcid.org/0000-0003-1644-2367)

**Azizah M. Malebari** – Department of Pharmaceutical Chemistry, College of Pharmacy, King Abdulaziz University, Jeddah 21589, Saudi Arabia

**Mohamed S. Nafie** – Department of Chemistry, Faculty of Science, Suez Canal University, Ismailia 41522, Egypt; [orcid.org/0000-0003-4454-6390](https://orcid.org/0000-0003-4454-6390)

**Adnan A. Bekhit** – Department of Pharmaceutical Chemistry, Faculty of Pharmacy, Alexandria University, Alexandria 21521, Egypt; Pharmacy Program, Allied Health Department, College of Health and Sport Sciences, University of Bahrain, Zallaq, Kingdom of Bahrain

**Amgad Alboby** – Department of Pharmaceutical Chemistry, Faculty of Pharmacy, The British University in Egypt (BUE), Cairo 11837, Egypt; The Center for Drug Research and Development (CDRD), Faculty of Pharmacy, The British University in Egypt, Cairo 11837, Egypt

**Alamgir Khan** – H.E.J. Research Institute of Chemistry, International Center for Chemical and Biological Sciences, University of Karachi, Karachi 75270, Pakistan

**Zaheer Ul-Haq** – H.E.J. Research Institute of Chemistry, International Center for Chemical and Biological Sciences and Dr. Panjwani Center for Molecular Medicine and Drug

Research, International Center for Chemical and Biological Sciences, University of Karachi, Karachi 75270, Pakistan  
**Matti Haukka** – Department of Chemistry, University of Jyväskylä, FI-40014 Jyväskylä, Finland; [orcid.org/0000-0002-6744-7208](https://orcid.org/0000-0002-6744-7208)

**Beatriz G. de la Torre** – KwaZulu-Natal Research Innovation and Sequencing Platform (KRISP), School of Laboratory Medicine and Medical Sciences, College of Health Sciences, University of KwaZulu-Natal, Durban 4041, South Africa; Peptide Science Laboratory, School of Chemistry and Physics, University of KwaZulu-Natal, Durban 4000, South Africa; [orcid.org/0000-0001-8521-9172](https://orcid.org/0000-0001-8521-9172)

Complete contact information is available at:

<https://pubs.acs.org/doi/10.1021/acsomega.2c03079>

### Author Contributions

The strategy was designed by A.E.-F., A.B., B.G.T., and F.A. Experimental work was performed by I.S.; biological studies were performed by A.M.M., M.S.N., A.B., A.A., and Z.U., and X-ray study was performed by M.H. All of the authors discussed the results and prepared the manuscript. All authors approved the final version of the manuscript.

### Notes

The authors declare no competing financial interest.

## ■ ACKNOWLEDGMENTS

The authors would like to extend their sincere appreciation to the Researchers Supporting Project (RSP-2021/64), King Saud University, Riyadh, Saudi Arabia. This work was partially funded by National Research Foundation (NRF) (Blue Sky's Research Programme No. 120386).

## ■ REFERENCES

- (1) Dugan, J.; Pollyea, D. Enasidenib for the treatment of acute myeloid leukemia. *Expert Rev. Clin Pharmacol.* **2018**, *11*, 755–760.
- (2) Yan, W.; Zhao, Y.; He, J. Anti-breast cancer activity of selected 1,3,5-triazines via modulation of EGFR-TK. *Mol. Med. Rep.* **2018**, *18*, 4175–4184.
- (3) Cascioferro, S.; Parrino, B.; Spanò, V.; Carbone, A.; Montalbano, A.; Barraja, P.; Diana, P.; Cirrincione, G. 1,3,5-Triazines: A promising scaffold for anticancer drugs development. *Eur. J. Med. Chem.* **2017**, *142*, 523–549.
- (4) Sharma, A.; Sheyi, R.; De La Torre, B. G.; El-Faham, A.; Albericio, F. S-triazine: A privileged structure for drug discovery and bioconjugation. *Molecules* **2021**, *26*, 864–880.
- (5) Hu, J.; Zhang, Y.; Tang, N.; Lu, Y.; Guo, P.; Huang, Z. Bioorganic & Medicinal Chemistry Discovery of novel 1, 3, 5-triazine derivatives as potent inhibitor of cervical cancer via dual inhibition of PI3K/mTOR. *Bioorg. Med. Chem.* **2021**, *32*, 115997–116012.
- (6) Malebari, A. M.; Abd Alhameed, R.; Almarhoon, Z.; Farooq, M.; Wadaan, M. A. M.; Sharma, A.; de la Torre, B. G.; Albericio, F.; El-Faham, A. The Antiproliferative and Apoptotic Effect of a Novel Synthesized S -Triazine Dipeptide Series, and Toxicity Screening in Zebrafish Embryos. *Molecules* **2021**, *26*, 1170–1185.
- (7) Mehmood, Y.; Anwar, F.; Saleem, U.; Hira, S.; Ahmad, B.; Bashir, M.; Imtiaz, M. T.; Najm, S.; Ismail, T. Compound against mammary glands cancer: Via down-regulating the hormonal, inflammatory mediators, and oxidative stress. *Life Sci.* **2021**, *285*, 119994–120008.
- (8) Keldsen, N.; Havsteen, H.; Vergote, I.; Bertelsen, K.; Jakobsen, A. Altretamine (hexamethylmelamine) in the treatment of platinum-resistant ovarian cancer: A phase II study. *Gynecol Oncol.* **2003**, *88*, 118–122.
- (9) Kim, E. S. Enasidenib: First Global Approval. *Drugs* **2017**, *77*, 1705–1711.

- (10) Shor, R. E.; Dai, J.; Lee, S.; Pisarsky, L.; Matei, I.; Lucotti, S.; Lyden, D.; Bissell, M. J.; Ghajar, C. M. The PI3K/mTOR inhibitor Gedatolisib eliminates dormant breast cancer cells in organotypic culture, but fails to prevent metastasis in preclinical settings. *Mol. Oncol.* **2022**, *16*, 130–147.
- (11) Bhat, H. R.; Masih, A.; Shaky, A.; Kumar, S. Design, synthesis, anticancer, antibacterial, and antifungal evaluation of 4-aminoquinoline-1, 3, 5-triazine derivatives. *J. Heterocyclic Chem.* **2020**, *57*, 390–399.
- (12) Raghu, M. S.; Pradeep Kumar, C. B.; Prashanth, M. K.; Yogesh Kumar, K.; Prathibha, B. S.; Kanthimathi, G.; Alissa, S. A.; Alghulikh, H. A.; Osman, S. M. Novel 1,3,5-triazine-based pyrazole derivatives as potential antitumor agents and EGFR kinase inhibitors: synthesis, cytotoxicity, DNA binding, molecular docking and DFT studies. *New J. Chem.* **2021**, *45*, 13909–13924.
- (13) Van Dort, M. E.; Galbán, S.; Wang, H.; Sebolt-Leopold, J.; Whitehead, C.; Hong, H.; Rehemtulla, A.; Ross, B. D. Dual inhibition of allosteric mitogen-activated protein kinase (MEK) and phosphatidylinositol 3-kinase (PI3K) oncogenic targets with a bifunctional inhibitor. *Bioorg. Med. Chem.* **2015**, *23*, 1386–1394.
- (14) Wang, Y.; Tortorella, M. Molecular design of dual inhibitors of PI3K and potential molecular target of cancer for its treatment: A review. *Eur. J. Med. Chem.* **2022**, *228*, 114039.
- (15) Zoncu, R.; Efeyan, A.; Sabatini, D. M. mTOR: From growth signal integration to cancer, diabetes and ageing. *Nat. Rev. Mol. Cell Biol.* **2011**, *12*, 21–35.
- (16) Beaufils, F.; Cmiljanovic, N.; Cmiljanovic, V.; Bohnacker, T.; Melone, A.; Marone, R.; Jackson, E.; Zhang, X.; Sele, A.; Borsari, C.; Mestan, J.; Hebeisen, P.; Hillmann, P.; Giese, B.; Zvelebil, M.; Fabbro, D.; Williams, R. L.; Rageot, D.; Wymann, M. P. 5-(4-(6-Dimorpholino-1,3,5-triazin-2-yl)-4-(trifluoromethyl)pyridin-2-amine (PQR309), a Potent, Brain-Penetrant, Orally Bioavailable, Pan-Class I PI3K/mTOR Inhibitor as Clinical Candidate in Oncology. *J. Med. Chem.* **2017**, *60*, 7524–7538.
- (17) Hu, J.; Zhang, Y.; Tang, N.; Lu, Y.; Guo, P.; Huang, Z. Discovery of novel 1,3,5-triazine derivatives as potent inhibitor of cervical cancer via dual inhibition of PI3K/mTOR. *Bioorg. Med. Chem.* **2021**, *32*, 115997–116011.
- (18) Patil, V.; Noonikara-poyil, A.; Joshi, S. D.; Patil, S. A.; Patil, S. A.; Lewis, A. M.; Bugarin, A. Synthesis, molecular docking studies, and in vitro evaluation of 1,3,5-triazine derivatives as promising antimicrobial agents. *J. Mol. Struct.* **2020**, *1220*, 128687–128695.
- (19) Kumar, R.; Singh, A. D.; Singh, J.; Singh, H.; Roy, R. K.; Chaudhary, A. 1,2,3-Triazine Scaffold as a Potent Biologically Active Moiety: A Mini Review. *Rev. Med. Chem.* **2014**, *14*, 72–83.
- (20) Shaky, A. Microwave assisted synthesis, docking and antimalarial evaluation of hybrid PABA-substituted. *J. Heterocyclic Chem.* **2020**, *57*, 2389–2399.
- (21) Asadi, P.; Alvani, M.; Hajhashemi, V.; Rostami, M.; Khodarahmi, G. Design, synthesis, biological evaluation, and molecular docking study on triazine based derivatives as anti-inflammatory agents. *J. Mol. Struct.* **2021**, *1243*, 130760–130770.
- (22) Marín-Ocampo, L.; Veloza, L. A.; Abonia, R.; Sepúlveda-Arias, J. C. Anti-inflammatory activity of triazine derivatives: A systematic review. *Eur. J. Med. Chem.* **2019**, *162*, 435–447.
- (23) Reddy, M. V. K.; Rao, K. Y.; Anusha, G.; Kumar, G. M.; Damu, A. G.; Reddy, K. R.; Shetti, N. P.; Aminabhavi, T. M.; Reddy, P. V. In-vitro evaluation of antioxidant and anticholinesterase activities of novel pyridine, quinoxaline and s-triazine derivatives. *Environ. Res.* **2021**, *199*, 111320.
- (24) Lolak, N.; Akocak, S.; Turkes, C.; Taslimi, P.; Isik, M.; Beydemir, S.; Gulcin, I.; Durgun, M. Synthesis, characterization, inhibition effects, and molecular docking studies as acetylcholinesterase,  $\alpha$ -glycosidase, and carbonic anhydrase inhibitors of novel benzenesulfonamides incorporating 1,3,5-triazine structural motif. *Bioorg. Chem.* **2020**, *100*, 103897–103907.
- (25) Viira, B.; Selyutina, A.; García-Sosa, A. T.; Karonen, M.; Sinkkonen, J.; Merits, A.; Maran, U. Design, discovery, modelling, synthesis, and biological evaluation of novel and small, low toxicity s-triazine derivatives as HIV-1 non-nucleoside reverse transcriptase inhibitors. *Bioorg. Med. Chem.* **2016**, *24*, 2519–2529.
- (26) Barakat, A.; El-Faham, A.; Haukka, M.; Al-Majid, A. M.; Soliman, S. M. s-Triazine pincer ligands: Synthesis of their metal complexes, coordination behavior, and applications. *Appl. Organomet. Chem.* **2021**, *35*, 1–112.
- (27) El-Mahdy, G. A.; Al-Rasheed, H. H.; Alshaikh, M.; Al-Lohedan, H. A.; El-Faham, A. 2,4-Dihydrazino-6-Morpholino-1,3,5-Triazine (DHMT) and 2,4-Dihydrazino-6-Piperidino-1,3,5-Triazine (DHPT) as promising corrosion inhibitors of steel in acidic media. *Int. J. Electrochem. Sci.* **2016**, *11*, S459–S472.
- (28) Sharma, A.; Ghabbour, H.; Khan, S. T.; de la Torre, B. G.; Albericio, F.; El-Faham, A. Novel pyrazolyl-s-triazine derivatives, molecular structure and antimicrobial activity. *J. Mol. Struct.* **2017**, *1145*, 244–253.
- (29) Abdellatif, K. R. A.; Abdelgawad, M. A.; Elshemy, H. A. H.; Alsayed, S. S. R.; Kamel, G. Synthesis and anti-inflammatory evaluation of new 1,3,5-triaryl-4,5-dihydro-1H-pyrazole derivatives possessing an aminosulphonyl pharmacophore. *Arch. Pharm. Res.* **2015**, *38*, 1932–1942.
- (30) Nehra, B.; Rulhania, S.; Jaswal, S.; Kumar, B.; Singh, G.; Monga, V. European Journal of Medicinal Chemistry Recent advancements in the development of bioactive pyrazoline derivatives. *Eur. J. Med. Chem.* **2020**, *205*, 112666–112699.
- (31) Murahari, M.; Mahajan, V.; Neeladri, S.; Kumar, M. S.; Mayur, Y. C. Ligand based design and synthesis of pyrazole based derivatives as selective COX-2 inhibitors. *Bioorg. Chem.* **2019**, *86*, S83–S97.
- (32) Tessmann, J. W.; Buss, J.; Beghini, K. R.; Berneira, L. M.; Paula, F. R.; de Pereira, C. M. P.; Collares, T.; Seixas, F. K. Antitumor potential of 1-thiocarbamoyl-3,5-diaryl-4,5-dihydro-1H-pyrazoles in human bladder cancer cells. *Biomed. Pharmacother.* **2017**, *94*, 37–46.
- (33) Naim, M. J.; Alam, O.; Nawaz, F.; Alam, M. J.; Alam, P. Current status of pyrazole and its biological activities. *J. Pharm. Bioallied Sci.* **2016**, *8*, 2–17.
- (34) Ilango, K.; Valentina, P. *Textbook of Medicinal Chemistry*, 1st ed.; Keerthi Publishers: Chennai, India, 2007; pp 327–333.
- (35) Farooq, M.; Sharma, A.; Almarhoon, Z.; Al-Dhfyhan, A.; El-Faham, A.; Taha, N. A.; Wadaan, M. A. M.; Torre, B. G. d. la; Albericio, F. Design and synthesis of mono- and di-pyrazolyl-s-triazine derivatives, their anticancer profile in human cancer cell lines, and in vivo toxicity in zebrafish embryos. *Bioorg. Chem.* **2019**, *87*, 457–464.
- (36) Moreno, L. M.; Quiroga, J.; Abonia, R.; Ramírez-Prada, J.; Insuasty, B. Synthesis of New 1,3,5-Triazine-Based 2-Pyrazolines as Potential Anticancer Agents. *Molecules* **2018**, *23*, 1956–1975.
- (37) Mikhaylichenko, S. N.; Patel, S. M.; Dalili, S.; Chesnyuk, A. A.; Zaplshny, V. N. Synthesis and structure of new 1,3,5-triazine-pyrazole derivatives. *Tetrahedron Lett.* **2009**, *50*, 2505–2508.
- (38) Shawish, I.; Soliman, S. M.; Haukka, M.; Dalbahi, A.; Barakat, A.; El-Faham, A. Synthesis, and Molecular Structure Investigations of a New s-Triazine Derivatives Incorporating Pyrazole/Piperidine/Aniline Moieties. *Crystals* **2021**, *11*, 1500.
- (39) Heppner, D. E.; Gunther, M.; Wittlinger, F.; Laufer, S. A.; Eck, M. J. Structural Basis for EGFR Mutant Inhibition by Trisubstituted Imidazole Inhibitors. *J. Med. Chem.* **2020**, *63*, 4293–4305.
- (40) Srivastava, J. K.; Pillai, G. G.; Bhat, H. R.; Verma, A.; Singh, U. P. Design and discovery of novel monastrol-1,3,5-triazines as potent anti-breast cancer agent via attenuating Epidermal Growth Factor Receptor tyrosine kinase. *Sci. Rep.* **2017**, *7*, 5851.
- (41) Sarbassov, D. D.; Ali, S. M.; Sabatini, D. M. Growing roles for the mTOR pathway. *Curr. Opin. Cell Biol.* **2005**, *17*, 596–603.
- (42) Poulsen, A.; Williams, M.; Nagaraj, H. M.; William, A. D.; Wang, H.; Soh, C. K.; Xiong, Z. C.; Dymock, B. Structure-based optimization of morpholino-triazines as PI3K and mTOR inhibitors. *Bioorg. Med. Chem. Lett.* **2012**, *22*, 1009–1013.
- (43) Hassan, B.; Akcakanat, A.; Holder, A. M.; Meric-Bernstam, F. Targeting the PI3-Kinase/Akt/mTOR Signaling Pathway. *Surg. Oncol. Clin. N. Am.* **2013**, *22*, 641–664.
- (44) Lee, J. J. X.; Loh, K.; Yap, Y. S. PI3K/Akt/mTOR inhibitors in breast cancer. *Cancer Biol. Med.* **2015**, *12*, 342–354.

(45) Raghu, M. S.; Pradeep Kumar, C. B.; Prashanth, M. K.; Yogesh Kumar, K. B.; Prathibha, S.; Kanthimathi, G.; Alissa, S. A.; Alghulikah, H. A.; Osman, S. M. Novel 1,3,5-triazine-based pyrazole derivatives as potential antitumor agents and EGFR kinase inhibitors: synthesis, cytotoxicity, DNA binding, molecular docking and DFT studies. *New J. Chem.* **2021**, *45*, 13909–13924.